Astron. Astrophys. 327, 1222–1229 (1997)

ASTRONOMY AND ASTROPHYSICS

Aspects of the solar tachocline

J.R. Elliott

JILA, University of Colorado, Boulder, CO 80309-0440, USA

Received 26 March 1996 / Accepted 27 May 1997

Abstract. The splitting of the frequencies of p-mode multiplets enables information to be gained about the internal rotation of the sun. Such data have revealed a transition at the base of the convection zone from differential rotation similar to that observed at the surface to almost solid-body rotation in the radiative interior. This transition region, known as the tachocline, has been found to be relatively narrow and centred below the base of the convection zone. In this paper, the evolution of the transition region is investigated numerically. Without a large anisotropic viscosity, the depth to which it would spread in one solar age, under the assumption of a constant prescribed differential rotation at the base of the convection zone, is found to be greater than its extent as inferred from helioseismology. In the second part of the paper a highly anisotropic turbulent viscosity with a large horizontal component, as suggested by Spiegel & Zahn (1992), is assumed. In this case, a steady tachocline is formed in which the advection of angular momentum balances the Reynolds stresses. The horizontal component of turbulent viscosity required to match the thickness of the tachocline to that obtained by helioseismology is estimated to be $5 \times 10^5 \mathrm{cm}^2\mathrm{s}^{-1}$. The transport of helium is studied in this case and is found to yield a sound-speed increase similar to that required by helioseismology.

Key words: Sun: interior; rotation; oscilations

1. Introduction

The accurate measurement of the frequencies of solar p-modes has enabled much information to be gained about the distribution of angular momentum within the solar interior (Brown et al. 1989; Goode et al. 1991; Sekii 1991; Thompson et al. 1996). This has made the search for a good theoretical understanding of the processes at work within rotating stars all the more important.

The possible existence of a meridional circulation, which could transport material and angular momentum within the solar radiative interior, was first proposed by Eddington in the early part of this century. However, a consistent picture of the distribution of angular momentum to which the sun evolves has been difficult to ascertain. Tassoul & Tassoul (1982), amongst others, argued that the sun must evolve to a state where a balance exists between the transport of angular momentum by advection and its transport by turbulent viscosity. This turbulence could very well arise from shear instability (Spiegel & Zahn 1970), with other instabilities almost certainly playing a role.

A particularly interesting aspect of the solar angular-momentum distribution is the transition layer between the rigidly-rotating radiative interior, and the differentially-rotating convection zone. This layer, known as the tachocline, is believed to be an important component of the dynamo which is responsible for the solar cycle – its strong shear has the ability to transform a poloidal field into a strong toroidal field, which can rise up buoyantly through the convection zone and erupt on the solar surface as sunspots (Spiegel & Weiss 1980).

In this paper, the time evolution of differential rotation in the tachocline is studied by means of a numerical simulation, assuming the rotation rate at the base of the convection zone to be prescribed. The equations solved are similar to those of Spiegel & Zahn (1992). Various other simplifying assumptions are made, the details of which are described in Sect. 2.2. It is initially assumed that the flow is not highly anisotropic – in this case the differential rotation is found to spread far into the radiative interior. A highly anisotropic viscosity is then introduced in Sect. 5 – this has the effect of limiting the spreading of the differential rotation and establishing a balance between advection of angular momentum and transport by turbulent viscosity.

The effect of the corresponding circulation on the transport of helium is studied in Sect. 6. Helium originating in the convection zone, which has settled under gravity into the tachocline, is mixed back into the convection zone. This causes a reduction in the mean molecular weight in the tachocline, and a consequent increase in the sound speed there. Since helioseismic inversions in this region indicate a higher sound speed in the sun than in current models, mixing improves the agreement with such inversions.

Send offprint requests to: J.R. Elliott

2. Governing equations

2.1. Equations in a rotating frame

In order to describe differential rotation in the solar interior it is useful to write the equations of motion with respect to a frame rotating with angular velocity Ω. The equations of conservation of mass, momentum, and energy become

$$\frac{\partial \rho}{\partial t} + \nabla \cdot (\rho \boldsymbol{v}) = 0 , \tag{1}$$

$$\rho \left[\frac{\partial \boldsymbol{v}}{\partial t} + (\boldsymbol{v} \cdot \nabla)\boldsymbol{v} + 2\boldsymbol{\Omega} \times \boldsymbol{v} \right] = -\nabla p - \rho \nabla \Phi + \nabla \cdot ||\tau|| , \tag{2}$$

$$\rho T \left(\frac{\partial S}{\partial t} + \boldsymbol{v} \cdot \nabla S \right) = \nabla \cdot (\chi \nabla T) , \tag{3}$$

where ρ, T and p are the density, temperature and pressure respectively, $\boldsymbol{v}$ is the fluid velocity, S is the specific entropy, χ is the thermal conductivity, Φ is the gravitational potential, and $||\tau||$ is the turbulent stress tensor.

2.2. Assumptions

The equations are solved under the assumption that the mean structure and the large-scale flow are axisymmetric about the axis of rotation (the small-scale turbulence is certainly not). The system can therefore be described solely in terms of the spherical coordinates r and θ, where θ is the colatitude. The solution is sought in a spherical shell with the outer edge corresponding to the base of the convection zone.

All structure quantities, for example the pressure, p, are separated into a mean value on the sphere plus a perturbation:

$$p(r, \theta, t) = \overline{p}(r, t) + \widetilde{p}(r, \theta, t) , \tag{4}$$

where $\int \widetilde{p}(r, \theta, t) \sin\theta \, d\theta = 0$. The angular rotation rate, ω, is written as

$$\omega(r, \theta, t) = \frac{v_\phi}{r \sin\theta} = \overline{\omega}(r, t) + \widetilde{\omega}(r, \theta, t) , \tag{5}$$

where $\int \widetilde{\omega}(r, \theta, t) \sin^3\theta \, d\theta = 0$.

Equations (1)-(3) are solved under assumptions which are very similar to those employed by Spiegel & Zahn (1992). They are as follows:

1. The time scale of the flow is very much longer than the sound crossing time, and the circulation can therefore be calculated using the *anelastic* approximation, i.e. that $\nabla \cdot (\rho \boldsymbol{v}) = 0$. This cannot hold strictly as it would imply $\partial\rho/\partial t = 0$ which is clearly not the case. However, since the time scale of the circulation is very much shorter than the time scale on which the density is modified (the Eddington–Sweet time scale), $\partial\rho/\partial t$ may safely be neglected.
2. Since the time scale of the flow is long compared to the rotation time scale, the inertial and viscous forces are small compared to the Coriolis forces in the radial and latitudinal directions; in these two directions a geostrophic balance exists between the Coriolis force and the pressure gradient. Since no zonal pressure gradient can exist owing to the assumption of axisymmetry, the azimuthal Coriolis force *must* be balanced by inertial and viscous forces.
3. The oblateness in the figure of the sun caused by the centrifugal force is small enough that the level surfaces of the effective potential can be taken to be spheres, with a compensating thermal source term added to the energy equation (Zahn 1992),

$$\varepsilon_{ES} = \frac{L}{M} E_\Omega P_2(\cos\theta) , \tag{6}$$

where L and M are the solar luminosity and mass respectively, P_2 denotes the second Legendre polynomial, and in the case of uniform rotation, E_Ω may be represented as

$$E_\Omega = 2 \left(1 - \frac{\Omega^2}{2\pi G \rho} \right) \frac{\widetilde{g}}{\overline{g}} , \tag{7}$$

where $\Omega = |\boldsymbol{\Omega}|$. In the outer regions of a star, the non-spherically symmetric component of the gravitational acceleration may be represented as

$$\frac{\widetilde{g}}{\overline{g}} \approx \frac{4}{3} \left(\frac{\Omega^2 r^3}{GM} \right) . \tag{8}$$

4. Second derivatives of thermodynamic quantities are neglected, i.e. quantities like the specific heat at constant pressure, C_p, and the thermal conductivity, χ, are assumed to be constant. This leads to a linear, ideal-gas equation of state

$$\frac{\widetilde{p}}{\overline{p}} = \frac{\widetilde{T}}{\overline{T}} + \frac{\widetilde{\rho}}{\overline{\rho}} . \tag{9}$$

No explicit assumptions are made regarding the thickness, h, of the shell in which the simulation is performed. However the accuracy of the simulation is sensitive to h through the neglect of modifications to the background state caused by the changing $\overline{\omega}(r, t)$. Since the modification of the background state involves a displacement of the order of $h\overline{\omega}/\Omega$, which in turn reacts back on $\overline{\omega}(r, t)$ by an amount $h\overline{\omega}/r$, this approximation becomes progressively worse as the thickness of the shell increases. If the modification of the background state were included, the effect would be to reduce the pressure fluctuation, $\widetilde{p}$, and thereby also to reduce the predicted circulation velocity.

2.3. Simplified equations

Under the above assumptions, the radial component of the momentum equation reduces to

$$2r \sin^2\theta \, \Omega \, \widetilde{\omega} = \frac{1}{\overline{\rho}} \frac{\partial \widetilde{p}}{\partial r} + g \frac{\widetilde{\rho}}{\overline{\rho}} , \tag{10}$$

where g is the acceleration due to gravity, with g assumed to be a constant, prescribed function of radius, since the layers of interest are at a large distance from the solar core. The θ component of the momentum equation becomes

$$2r \sin\theta \cos\theta \, \Omega \, \widetilde{\omega} = \frac{1}{r\overline{\rho}} \frac{\partial \widetilde{p}}{\partial \theta} . \tag{11}$$

The ϕ component of the momentum equation, which expresses the balance between Coriolis, inertial, and viscous forces, becomes

$$r\sin\theta\frac{\partial\omega}{\partial t}+v_r\frac{\partial v_\phi}{\partial r}+v_\theta\frac{\partial v_\phi}{\partial\theta}+2\Omega\left(v_r\sin\theta+v_\theta\cos\theta\right)=$$
$$\frac{\sin^2\theta}{\overline{\rho}r^2}\frac{\partial}{\partial r}\left(\overline{\rho}\nu_V r^4\frac{\partial\omega}{\partial r}\right)+\frac{1}{r\sin^2\theta}\frac{\partial}{\partial\theta}\left(\nu_H\sin^3\theta\frac{\partial\omega}{\partial\theta}\right), \qquad (12)$$

where ν_H and ν_V are the horizontal and vertical components of the turbulent viscosity.

As a result of the anelastic approximation, the circulation in the spherical shell may be represented by a streamfunction Ψ,

$$\overline{\rho}r^2\sin\theta v_r=\frac{\partial\Psi}{\partial\theta}, \qquad (13)$$

$$\overline{\rho}r\sin\theta v_\theta=-\frac{\partial\Psi}{\partial r}, \qquad (14)$$

where v_r and v_θ are, respectively, the radial and tangential components of the velocity. Since the system is assumed to be axisymmetric about the axis of rotation as well as having reflective symmetry with respect to the equatorial plane (a consequence of the symmetry of the imposed boundary conditions), v_θ should vanish at $\theta = 0$ and $\theta = \pi/2$. Eq. (14) implies that Ψ must also vanish at these values of θ. Integrating Eq. (13) with respect to θ, this condition corresponds to the requirement that $\int v_r\sin\theta d\theta = 0$, or that there is no net inward or outward mass flux.

The energy equation consists of a spherically-averaged part, neglected in this paper, and a perturbation given by

$$\frac{\partial\tilde{T}}{\partial t}=-v_r\overline{T}\frac{d\ln p}{dr}\left(\nabla_{ad}-\nabla\right)+\frac{1}{\overline{\rho}C_p}\left[\frac{1}{r^2}\frac{\partial}{\partial r}\left(\chi r^2\frac{\partial\tilde{T}}{\partial r}\right)\right.$$
$$\left.+\frac{1}{r^2\sin\theta}\frac{\partial}{\partial\theta}\left(\chi\sin\theta\frac{\partial\tilde{T}}{\partial\theta}\right)+\overline{\rho}\varepsilon_{ES}\right], \qquad (15)$$

where ∇ is the temperature gradient $d\ln T/d\ln p$, and ∇_{ad} is the thermodynamic derivative $\partial\ln T/\partial\ln p$ at constant specific entropy. The potential singularity in v_r caused by $\nabla_{ad}-\nabla$ passing through zero is avoided by locating the base of the convection zone at the point where the convective heat flux becomes negligible. Owing to convective penetration, this is below the point where $\nabla = \nabla_{ad}$, and the stratification is therefore subadiabatic in the whole computational domain.

After about one thermal relaxation time, a balance is struck between the terms on the right-hand side of this equation, and the time derivative on the left-hand side may be neglected. It is not strictly zero, but since the system evolves on a time scale comparable with the local Eddington–Sweet time (Spiegel & Zahn 1992), it is small enough that the terms on the right balance almost perfectly.

2.4. Boundary conditions

Boundary conditions are imposed at the inner and outer edges of the region of solution. The system is fourth order and therefore four boundary conditions are required. The rotation rate is assumed to be prescribed by the convection zone above, and to have a form corresponding to that inferred from helioseismology. An inversion has recently been carried out for the solar internal rotation using splitting data from the GONG network (Thompson et al. 1996). At the base of the convection zone, this inversion leads to the following expression for Ω_{bcz}:

$$\frac{\Omega_{bcz}}{2\pi}=456-72\cos^2\theta-42\cos^4\theta\ \text{nHz}. \qquad (16)$$

This is used to give the outer boundary condition on ω,

$$\Omega+\omega=\Omega_{bcz}\ \text{at}\ r=r_{bcz}, \qquad (17)$$

where r_{bcz} is the radius of the base of the convection zone. Ω is chosen to be the rotation rate of the radiative interior below the tachocline – helioseismic inversions indicate that this value is equal to the rotation rate of the convection zone at a latitude of about 30°, corresponding to $\Omega/2\pi \approx 437$nHz.

The second outer boundary condition is derived from the requirement that the partial derivative of the rotation rate with respect to radius be continuous. Since helioseismic inversions indicate that the rotation rate depends little on radius deep within the convection zone, this boundary condition becomes:

$$\frac{\partial\omega}{\partial r}=0\ \text{at}\ r=r_{bcz}. \qquad (18)$$

The last two boundary conditions,

$$\omega=\frac{\partial\omega}{\partial r}=0, \qquad (19)$$

are imposed at the inner edge of the region of solution.

3. The solution

3.1. Numerical method

The evolution of the rotation rate $\omega(r,\theta,t)$ with time is studied numerically. Eqs. (10)-(15) are solved using finite differences to represent partial derivatives with respect to r and θ, and using a first-order explicit scheme to carry out the evolution in time. A uniformly spaced grid, with spacings Δr and $\Delta\theta$, is set up with equal numbers of points in the r and θ directions. r is chosen to vary from $r_{bcz}/2$ to r_{bcz}, while θ varies from 0 to $\pi/2$.

Initially, Eq. (11) is integrated to find $\tilde{p}(r,\theta,t)$ in terms of $\omega(r,\theta,t)$. Eq. (10) is then solved to find $\tilde{\rho}(r,\theta,t)$. $\tilde{T}(r,\theta,t)$ may then be obtained from the equation of state. After neglecting the time derivative in Eq. (15), the radial component of the velocity, v_r may be found by taking the Laplacian of $\tilde{T}(r,\theta,t)$.

The streamfunction $\Psi(r,\theta,t)$ is now evaluated. This is done by integrating Eq. (13) with respect to θ. The tangential component of the velocity, v_θ, may then be evaluated using Eq. (14). Finally, the rotation rate is updated using Eq. (12). The advective terms (the second and third terms on the left-hand side of this equation) are included, but turn out to be small in comparison with the Coriolis term (the last term on the left-hand side), since the Rossby number (the ratio of the advective term to the Coriolis acceleration) is small (Spiegel & Zahn 1992).

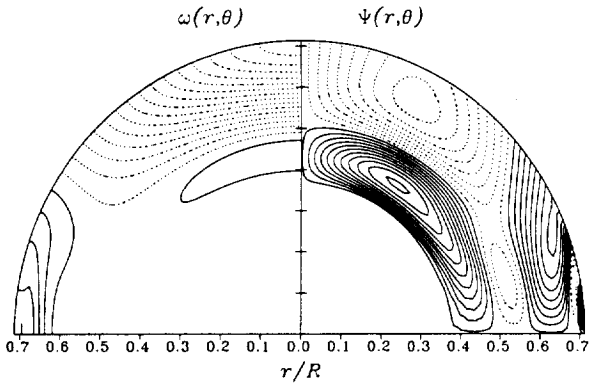

Fig. 1. The radiative spreading of differential rotation imposed at the edge of the radiative zone after one solar age. The left-hand quadrant shows contours of $\omega(r,\theta)$ with solid contours denoting prograde differential rotation, while the right-hand quadrant shows contours of the streamfunction $\Psi(r,\theta)$, with solid contours corresponding to clockwise circulation. The rotation of the base of the convection zone is here chosen to match that of the deep radiative interior at a latitude of approximately 30°.

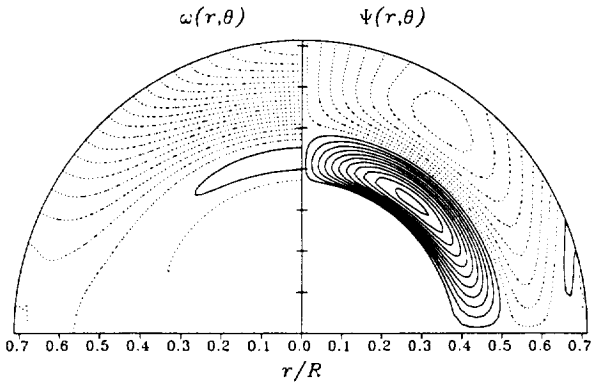

Fig. 2. As in Fig. 1, but with the boundary condition on ω at the base of the convection zone given in this case by Eq. (21).

The stability of this explicit time-evolution scheme is determined by the condition that the time step, Δt, should be shorter than the time for the differential rotation to spread radially a distance Δr,

$$\Delta t < \tau_{\rm ES} \left(\frac{\Delta r}{r} \right)^4 , \tag{20}$$

where $\tau_{\rm ES}$ is the local Eddington–Sweet time.

3.2. *Reference model*

The spherically-averaged values of p, ρ and T, along with the values of χ, C_p and g, are derived from a reference solar model (γ is assumed to take the ideal-gas value of 5/3). This reference model is constructed using the MHD equation of state (Mihalas et al. 1988) and the OPAL opacities (Iglesias & Rogers 1991) with an assumed heavy-element abundance of $Z = 0.02$. The assumed solar age is 4.6×10^9 years. Since the outcome of the current calculation is not particularly sensitive to the details of the reference model, discussion of other details of its construction are deferred.

3.3. *Initial conditions*

The initial conditions chosen for all simulations are $\omega(r, \theta, t = 0) = 0$. Since there is no way of knowing what the actual initial conditions should be in the solar case, there is an implicit assumption that the results obtained are not particularly sensitive to the initial conditions.

4. Radiative spreading

In this section, the turbulent viscosity is assumed not to be highly anisotropic. As a consequence of this, the horizontal transport of angular momentum, the last term in Eq. (12), may be neglected in comparison with the vertical transport as long as the tachocline is not too thick. Assuming the vertical transport term to be small also, the result of the numerical calculation described is shown in Fig. 1.

As can be seen, after one solar age, the transition region from differential rotation to rigid rotation has spread significantly into the radiative interior. Another feature of note is that the contours of the streamfunction Ψ, shown in the right-hand quadrant, are nearly parallel to the axis of rotation at the edge of the region of solution. This is because the imposed rotation law at the base of the convection zone forces the streamlines to be parallel to lines of constant specific angular momentum; since the latter are almost parallel to the axis of rotation, owing to the ratio $\Delta\Omega/\Omega$ being relatively small, the streamlines must also be nearly parallel to the axis of rotation.

A second calculation is performed under the assumptions of the work of Spiegel & Zahn (1992); in this analytical study, the radial component of the velocity was neglected in determining the evolution of the differential rotation, on the grounds that in a thin shell it would be small in comparison with the tangential component. This approximation allowed the equations to be separated in the r and θ directions, with the caveat that ω was forced to be zero at $\theta = \pi/2$. To test the effect of this restriction, a numerical simulation is carried out choosing

$$\omega(r_{\rm bcz}, \theta, t) = -72\cos^2\theta - 42\cos^4\theta \ {\rm nHz} , \tag{21}$$

in accord with Eq. (16). The result of this second simulation is shown in Fig. 2.

The depth to which differential rotation imposed at the edge of the radiative interior would diffuse in one solar age is seen to be roughly $0.2R_\odot$ in the cases shown in Fig. 1 and Fig. 2. This is somewhat smaller than the value obtained by the analytical calculation of Spiegel & Zahn (1992), namely about $0.2625R_\odot$, but still conflicts with the helioseismic determination of tachocline thickness and depth carried out by Kosovichev (1996). In the latter paper, a depth of $0.692 \pm 0.005R_\odot$ and a thickness of $0.09 \pm 0.04R_\odot$ were obtained by fitting a

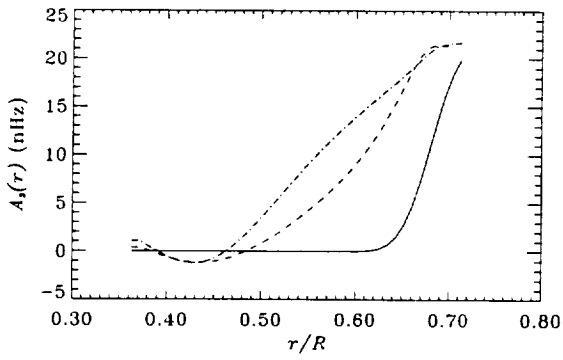

Fig. 3. The function $A_3(r)$ for the cases shown in Fig. 1 (dashed line) and Fig. 2 (dot-dashed line), and the form deduced by helioseismology (solid line).

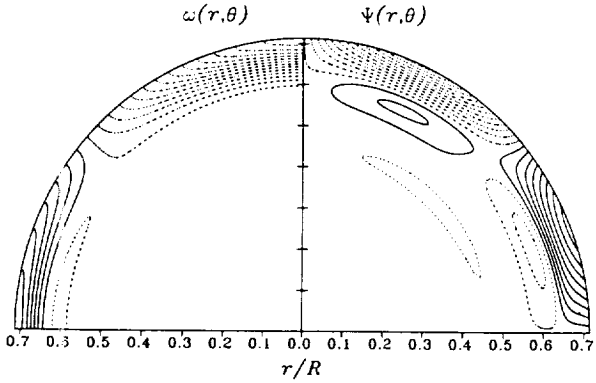

Fig. 4. The steady state reached when the advection of angular momentum by the meridional circulation balances the Reynolds stresses. The horizontal component of the turbulent viscosity is here chosen to be $5 \times 10^4 \mathrm{cm}^2\mathrm{s}^{-1}$, while the ratio $\nu_H/\nu_V = 1000$.

differential-rotation profile parameterized by depth and thickness to the solar p-mode splitting coefficients. In order to contrast the results of the radiative spreading described here with the results of helioseismology, the function $A_3(r)$, introduced by Kosovichev (1996) as the coefficient of the associated Legendre polynomial $P_3^1(\cos\theta)$ in an expansion for the rotation rate, is calculated for the two cases described in this section and compared with his parameterized best fit to the solar p-mode splittings. This particular coefficient was investigated by Kosovichev (1996) on the grounds that it is especially sensitive to the variation of angular rotation rate in the solar tachocline. Fig. 3 represents this comparison; the dashed line shows the case of interior rotation matching convection-zone rotation at a latitude of 30°, the dot-dashed line shows the case where ω is zero at the equator, while the solid line shows the best fit to the helioseismology data determined by Kosovichev (1996).

The spreading predicted by the results of these simple calculations is seen to be much greater than that determined observationally. In addition, it was here assumed that Ω was constant over the whole life time of the sun. In reality, the sun has been slowing down due to the braking effect of the solar wind, and was rotating faster in the past. The spreading would be increased if this slowing down was taken into account, making the discrepancy between the predictions of this model and observations even greater. Some way needs to be found of inhibiting the spreading of the tachocline into the radiative interior.

5. Anisotropic turbulent viscosity

Spiegel & Zahn (1992) suggested that strongly anisotropic turbulence could inhibit the spreading of the transition region into the radiative interior of the sun, and that in the solar tachocline a balance may exist between the advection of angular momentum by the circulation and the Reynolds stresses acting on the horizontal shear. Since the thickness of the tachocline would depend on the horizontal component of the turbulent viscosity, a knowledge of the thickness would enable this component to be estimated.

When

$$\frac{\nu_H}{\nu_V} \gg \left(\frac{r_{bcz}}{h}\right)^2 , \tag{22}$$

as may be the case when the stable stratification of the subconvective layers produces strongly anisotropic turbulence, the first term on the right-hand side of Eq. (12) may be neglected to give:

$$r\sin\theta\frac{\partial\omega}{\partial t} + v_r\frac{\partial v_\phi}{\partial r} + v_\theta\frac{\partial v_\phi}{\partial\theta} = -2\Omega\,(v_r\sin\theta + v_\theta\cos\theta) + \frac{1}{r\sin^2\theta}\frac{\partial}{\partial\theta}\left(\nu_H\sin^3\theta\frac{\partial\omega}{\partial\theta}\right) . \tag{23}$$

Once a balance has been established between the Coriolis and viscous forces (the two terms on the right-hand side of this equation), a steady state is reached. An example of such a steady state is shown in Fig. 4, which corresponds to a horizontal turbulent viscosity of $5 \times 10^4 \mathrm{cm}^2\mathrm{s}^{-1}$, and a ratio $\nu_H/\nu_V = 1000$. This ratio is sufficiently large that the criterion given by Eq. (22) is met.

The rotation rate at the base of the convection zone matches that of the deep radiative interior at a latitude of approximately 40°, much as predicted by the analytical calculation of Spiegel and Zahn (1992). The circulation also shows the octopolar configuration that they described, with two cells in each hemisphere. The thickness of the tachocline may be compared with the approximate formula given in that paper.

$$h = 20\,000\,(\kappa/\nu_H)^{\frac{1}{2}}\ \mathrm{km} , \tag{24}$$

where $\kappa = \chi/\bar{\rho}C_p$. Given $\nu_H = 5 \times 10^4 \mathrm{cm}^2\mathrm{s}^{-1}$ and using the value of κ from the base of the convection zone, this formula predicts a thickness of about 90 000km, or $0.13R_\odot$. This is somewhat larger than the tachocline thickness shown by our numerical calculation for this value of ν_H (approximately $0.1R_\odot$). The discrepancy reflects the fact that the approximate formula (24) was obtained under the assumption that the tachocline is vanishingly thin and that ω varies much more rapidly with radius than do other structure variables; when allowance is made

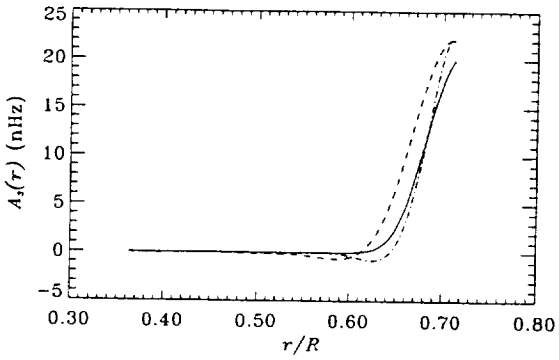

Fig. 5. The function $A_3(r)$ in the case of strongly anisotropic turbulent viscosity. The dashed line corresponds to $\nu_H = 5 \times 10^4 \mathrm{cm^2 s^{-1}}$, the dot-dashed line corresponds to $\nu_H = 5 \times 10^5 \mathrm{cm^2 s^{-1}}$, while the solid line corresponds to the form deduced by helioseismology.

for the variation of the background state with depth, as in this numerical calculation, the tachocline is found to be thinner than predicted by Eq. (24).

Fig. 5 shows the comparison between the function $A_3(r)$ for two models with strongly anisotropic turbulent viscosity (but different values of this viscosity) and that derived by Kosovichev (1996) from helioseismology. The dashed line shows $A_3(r)$ corresponding to the case shown in Fig. 4, while the dot-dashed line shows the same function for a horizontal turbulent viscosity ten times larger ($5 \times 10^5 \mathrm{cm^2 s^{-1}}$). The solid line shows the value obtained from helioseismology.

The better fit to the helioseismically deduced $A_3(r)$ is obtained with the higher value of $5 \times 10^5 \mathrm{cm^2 s^{-1}}$ for the horizontal turbulent viscosity plotted in Fig. 5. This value is significantly smaller than the lower bound of $1.5 \times 10^8 \mathrm{cm^2 s^{-1}}$ stated by Zahn (1992) based on Eq. (24). If a tachocline thickness of $0.1 R_\odot$ or 70 000km were presumed, then Eq. (24) would require the ratio κ/ν_H to be approximately 150. κ is approximately $2 \times 10^7 \mathrm{cm^2 s^{-1}}$ at the base of the convection zone, leading to $\nu_H \approx 10^5 \mathrm{cm^2 s^{-1}}$. The estimate of $1.5 \times 10^8 \mathrm{cm^2 s^{-1}}$ as a lower limit for ν_H would thus appear to be wrong, as it would lead to a tachocline several times narrower than the resolution of helioseismic inversions for the rotation rate.

Zahn (1992) used this limit to argue that if all the energy going into turbulent motions (as calculated from the shear implied by helioseismic measurements) were dissipated by viscosity on a small scale, then the vertical component of the turbulent viscosity required would imply a turbulent diffusivity too large to tolerate the observed surface abundance of lithium. This finding may simply be a consequence of the overestimate of the horizontal component of the turbulent viscosity.

The thickness of the tachocline in Fig. 4 shows a clear variation with latitude. There is some evidence in helioseismic inversions for rotation rate (Thompson et al. 1996) for such a variation being present in the sun, giving additional support to this theoretical description of the solar tachocline. The actual magnitude of the variation has yet to be quantified, and awaits more accurate determination of p-mode frequency splittings.

Under the assumption of no net torque at the base of the convection zone, models of the solar tachocline with strongly anisotropic viscosity predict a value of about 416nHz $\approx 0.91\Omega_e$ for the rotation rate of the solar radiative interior (Ω_e is the equatorial rotation rate); the value is determined solely by the imposed rotation law at the base of the convection zone, a dependence which has been described analytically by Spiegel & Zahn (1992). This differs from the current best helioseismic estimates, e.g. from GONG data, of about 435nHz $\approx 0.95\Omega_e$. Thus, in this model, the rotation rate of the radiative interior matches that of the convection zone at a latitude of about 40°, while helioseismology indicates that the two are equal at a latitude of nearer 30° in the sun.

In the presence of a torque, such as could be produced by angular-momentum loss associated with the solar wind, it might be expected that a large differential rotation would be set up, as suggested by Zahn (1992). Since helioseismic inversions indicate that there is no such differential rotation in the radiative interior, some mechanism must inhibit this process. It has been suggested by Rosner & Weiss (1985) and Mestel & Weiss (1987) that a weak connected magnetic field may cause the solar interior to rotate uniformly. Alternatively, Zahn (1994) has suggested that gravity waves excited by penetrative convection may transport angular momentum radially and help to enforce uniform rotation. The relative importance of such processes may become clearer as more detailed helioseismic data become available.

6. Mixing in the turbulent tachocline

Recent helioseismic inversions for the sound speed in the tachocline show a higher ($\delta c^2/c^2 \approx 0.004$) value in the sun than in the latest models. These models incorporate gravitational helium settling (Michaud & Proffitt 1993), which causes the helium abundance to increase with depth below the base of the convection zone. It has been suggested that the discrepancy could be due to the circulation in the turbulent tachocline mixing helium back into the convection zone, thus reducing the mean molecular weight in the tachocline and thereby increasing the sound speed.

In order to test this theory, the evolution of helium abundance is investigated using a model incorporating both gravitational settling and advection of helium. The circulation responsible for this advection is assumed to be that associated with a steady-state tachocline having $\nu_H = 5 \times 10^5 \mathrm{cm^2 s^{-1}}$; it is additionally assumed that the circulation has not changed with time. A diffusion term is included to make the solution smooth at the interface between the tachocline and the convection zone; the diffusion coefficient drops exponentially with depth below the base of the convection zone (with e-folding distance $0.01 R_\odot$), where it has a value of $200 \mathrm{cm^2 s^{-1}}$. The horizontal turbulent diffusion (corresponding to ν_H) of helium is not included. The mass of the convection zone is assumed to decrease linearly with time up to the present-day solar age from an initial value of $0.0256 M_\odot$ to a present-day value of $0.0183 M_\odot$. This linear trend, as well as the initial and final masses, are derived from the evolution of a standard solar model.

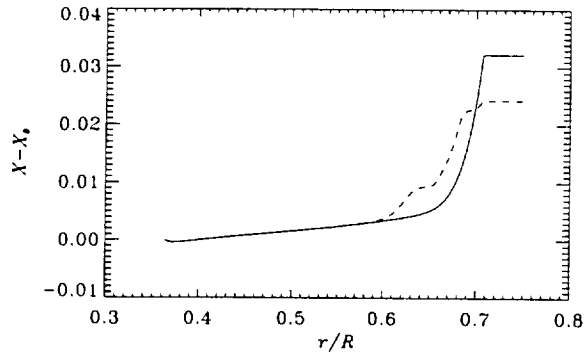

Fig. 6. The spherically-averaged hydrogen profiles obtained without advection of helium (solid line) and with advection (dashed line).

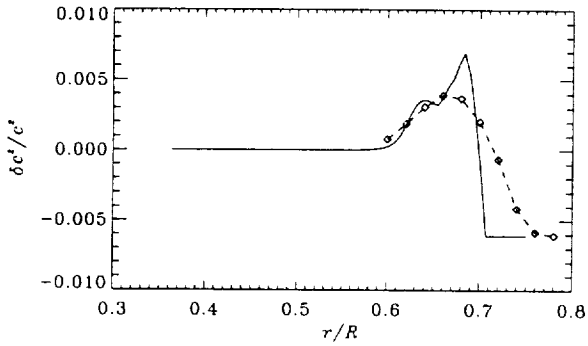

Fig. 7. The difference in sound speed between a model with advection by the tachocline circulation and a model without such advection (solid line); the diamonds (joined by the dashed line) show this quantity convolved with Gaussian functions having widths corresponding to those of optimally-localized averaging kernels from helioseismic inversions.

The result of the calculation is presented in Fig. 6. The solid line shows the spherically-averaged hydrogen abundance, X (after subtraction of the initial abundance, X_0), without advection by the circulation, while the dashed line shows the same quantity when advection is included. Without advection, the increase in convection-zone hydrogen abundance by the present day, 0.032, agrees reasonably well with that given by more detailed evolution calculations that include helium settling. When advection is included, helium is mixed back into the convection zone and the increase in convection-zone hydrogen abundance is reduced to 0.024. Advection also removes the steep gradient of hydrogen abundance just below the base of the convection zone, thus increasing the sound speed in this region and improving the agreement with helioseismic inversions. Looking more closely at the shape of the dashed line, the hydrogen abundance is seen to descend from the convection-zone value via two plateaus, which correspond to the two circulation cells seen in a radial cut through the streamfunction shown in Fig. 4.

The solid line in Fig. 7 shows the quantity $\delta c^2/c^2$, reflecting the difference in squared sound speed between the model with advection and that without. This quantity is assumed to be proportional to the fractional difference in mean molecular weight, which depends in turn on the chemical composition (a fully-ionized ideal gas is assumed). After convolution with Gaussian functions chosen to have widths reflecting those of optimally-localized averaging kernels used in helioseismic inversions, the dashed curve is obtained. The large hump in $\delta c^2/c^2$ below the base of the convection zone is very similar to that observed in helioseismic inversions for sound speed, and has an approximately correct amplitude (0.004). The mixing of helium back into the convection zone thus appears to be a good candidate for explaining the sound speed discrepancy in the region of the tachocline.

7. Conclusion

This paper has confirmed some of the findings of Spiegel & Zahn (1992). Without anisotropic viscosity, the differential rotation of the convection zone would diffuse into the radiative zone at too great a rate to comply with observations. When anisotropic viscosity is introduced, the spread of the differential rotation is inhibited, and a steady-state is reached in which advection of angular momentum balances Reynolds stresses. The rotation rate at the base of the transition region so formed is equal to the rotation rate of the base of the convection zone at a latitude of approximately 40°.

The simple viscous stress operator considered here is not the only case one could imagine. For instance, the coefficients of turbulent viscosity may vary with latitude, since turbulent motions are more strongly rotationally constrained at the poles than at the equator.

While the results presented here are mostly in agreement with those of Spiegel & Zahn (1992), the estimated value of the horizontal component of the turbulent viscosity, $5 \times 10^5 \mathrm{cm^2 s^{-1}}$, is significantly smaller than the lower bound given by Zahn (1992), and is only a few orders of magnitude larger than the microscopic viscosity. This implies very short characteristic length scales (10^4cm) at the velocities associated with convective motions, or very low velocities ($10^{-5}\mathrm{cm\,s^{-1}}$) at the length scale associated with the tachocline. It should be noted that given the uncertainty associated with current estimates of the tachocline thickness, and the weak dependence of this thickness on the horizontal turbulent viscosity, ν_H could in reality be significantly larger than the value obtained here.

Since the circulation associated with the steady-state tachocline advects helium, a certain amount of mixing occurs below the base of the convection zone. Numerical calculations taking into account the interaction between this mixing and gravitational settling show that the sound speed could be modified in such a way as to remove the discrepancy found in helioseismic inversions. This gives independent confirmation of the thickness of the tachocline as deduced from rotation-rate inversions.

In obtaining these results, several overall simplifying assumptions have been made. It has been assumed that the convection zone sets the boundary conditions for the radiative interior, which does not allow for any feedback of the radiative interior on the convection zone. The effects of convective over-

shoot have not been considered either – these would affect the boundary between the radiative interior and the convection zone over a region comparable with the pressure scale height. Turbulent transport of heat has also been neglected in comparison with radiative transport, an approximation which is valid so long as the tachocline is not too thin. A better model would consider the full interaction between the convection zone and radiative interior, allowing for the effects of penetrative convection and turbulent transport of heat – such a model would certainly be much more complex than that considered here.

What has emerged from the results presented here is the diagnostic potential of rotation-rate inversions using frequencies obtained from such experiments as MDI and GONG. By measuring the thickness of the tachocline, the variation of this thickness with latitude, and the interior rotation rate, many aspects of the dynamics of this fascinating region of the sun may be studied. The great improvement which may be expected in the accuracy of helioseismic measurements over the next several years will enable a much better understanding of the tachocline to be reached.

Acknowledgements. We thank J.-P. Zahn and J. Toomre for useful comments and the latter for suggestions on improving the presentation of the paper. This work is supported in part by the National Aeronautics and Space Administration through grants NAG5-2256 and NAG5-3077.

References

Brown, T.M., Christensen-Dalsgaard, J., Dziembowski, W.A., Goode, et al. 1989, ApJ, 343, 526
Goode, P.R., Dziembowski, W.A., Korzennik, S.G., Rhodes, E.J. 1991, ApJ, 367, 649
Iglesias, C.A., Rogers F.J. 1991, ApJ, 371, 408
Kosovichev, A.G. 1996, ApJ, 469, L61
Mestel, L., Weiss, N.O. 1987, MNRAS, 226, 123
Michaud, G., Proffitt, C.R. 1993, Inside the stars: Proc. of the 137th IAU Colloquium, 246
Mihalas, D., Däppen, W., Hummer, D.G. 1988, ApJ, 331, 815
Rosner, R., Wiess, N.O. 1985, Nat, 317, 790
Sekii, T. 1991, PASJ, 43, 381
Spiegel, E.A., Weiss, N.O. 1980, Nat, 287, 616
Spiegel, E.A., Zahn, J.-P. 1970, Comments Astrophys. Space Phys., 2, 178
Spiegel, E.A., Zahn, J.-P. 1992, A&A, 265, 106
Tassoul, J.-L., Tassoul, M. 1982, ApJS, 49, 317
Thompson, M.J., Toomre, J., The GONG Dynamics Inversion Team 1996, Sci, 272, 1300
Zahn, J.-P. 1992, A&A, 265, 115
Zahn, J.-P. 1994, A&A, 288, 829

This article was processed by the author using Springer-Verlag LaTeX A&A style file *L-AA* version 3.